ACS OMEGA

Open Access

http://pubs.acs.org/journal/acsodf

Article

Diels–Alder Cycloaddition of 2,5-Bis(hydroxymethyl)furan (BHMF) and *N*-Phenylmaleimide Derivatives

Harshit Shukla, Peerapong Promcharoen, Thinnaphat Poonsawat, Khetpakorn Chakarawet, Peerapong Chumkaeo, and Ekasith Somsook*

Cite This: *ACS Omega* 2024, 9, 36380–36388

Read Online

ACCESS | Metrics & More | Article Recommendations | Supporting Information

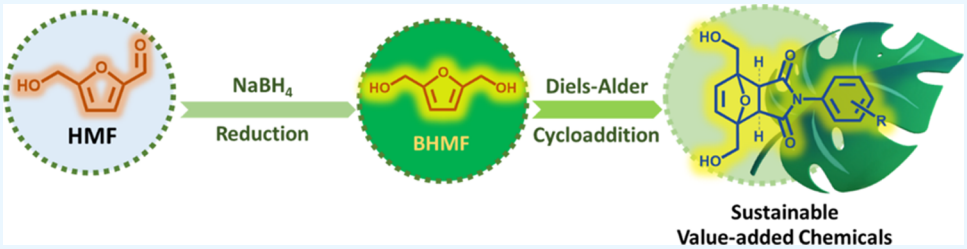

ABSTRACT: Currently, amidst atmospheric menace where natural calamities such as wildfire and floods are becoming more frequent than ever, biobased derivatives offer a sustainable alternative to conventional ways, for instance, petrochemical commodities. Biobased products, obtained from agricultural waste, including 5-(hydroxymethyl)furfural (HMF), 2,5-bis-(hydroxymethyl)furan (BHMF), and 2,5-furandicarboxylic acid (FDCA) are promising chemical platforms in the biorefinery, which is yet to be explored. The Diels–Alder cycloaddition of BHMF and *N*-phenylmaleimide derivatives under optimal reaction conditions is investigated in this report. First, HMF is reduced to BHMF in the presence of $NaBH_4$, and then the Diels–Alder reaction of BHMF and *N*-phenylmaleimide derivatives is investigated to produce Diels–Alder adducts. All novel compounds are synthesized in acceptable yields and effectively characterized by employing important techniques such as one-dimensional (1D) NMR spectroscopy (^{1}H, ^{13}C, DEPT-90, and DEPT- 135), two-dimensional (2D) NMR spectroscopy (^{1}H–^{1}H COSY, ^{1}H–^{13}C HSQC, and ^{1}H–^{13}C HMBC), IR spectroscopy, elemental analysis, mass spectrum (QTOF), and single-crystal X-ray diffraction (SC-XRD). Furthermore, this study underlines the necessity of sustainable synthetic methodologies and gives critical insights into the progress of ecologically friendly methodologies, providing a new avenue as a tunable precursor for the challenging functionalized polymer in the future.

INTRODUCTION

5-Hydroxymethylfurfural (5-HMF), an aromatic aldehyde derived from nonedible biomass such as corn cobs and sugar cane bagasse, has emerged as a promising sustainable substrate for various synthetic transformations in recent years.[1−7] As the world moves toward more sustainable and circular economic systems to mitigate climate change, there is an urgent need to transition from fossil-derived chemicals and materials to renewable biological feedstocks. In this regard, 5-hydroxymethylfurfural (5-HMF) has emerged as a versatile and promising biobased chemical platform for synthesizing commodity chemicals such as fuels,[8−11] plastics,[12,13] pharmaceuticals,[14−16] and specialty chemicals that have traditionally depended on fossil resources.[17−19] Furthermore, 5-hydroxymethylfurfural (HMF) has been highlighted as a vital compound for promoting sustainable development due to its extensive use as an essential chemical in biorefinery. Hydroxymethylfurfural (HMF) may be converted into 2,5-furandicarboxylic acid (FDCA), 2,5-dimethylfuran, 5-methylfurfural (MF), 5-methyl-2-furfuryl alcohol, and 2,5-bis(hydroxymethyl)furan (BHMF).[20−22] Among HMF-derived products, BHMF is a promising chemical platform for the synthesis of various macromolecules, polymers, and materials owing to the presence of a symmetrical diol functional group.[23−25] In this report, BHMF can be used as a starting material, presenting an innovative and nearly unexplored route with great potential by the Diels–Alder cycloaddition (Figure 1). In contrast to typical dienes, BHMF features two hydroxymethyl substitutions attached to a furan ring, which provide unique possibilities for stereochemical control and regioselectivity in cycloadditions.[26−28] However, the use of 2,5-bis-(hydroxymethyl)furan as a dienophile in Diels–Alder reactions

Received: April 21, 2024
Revised: June 7, 2024
Accepted: July 9, 2024
Published: August 14, 2024

https://doi.org/10.1021/acsomega.4c03804
ACS Omega 2024, 9, 36380–36388

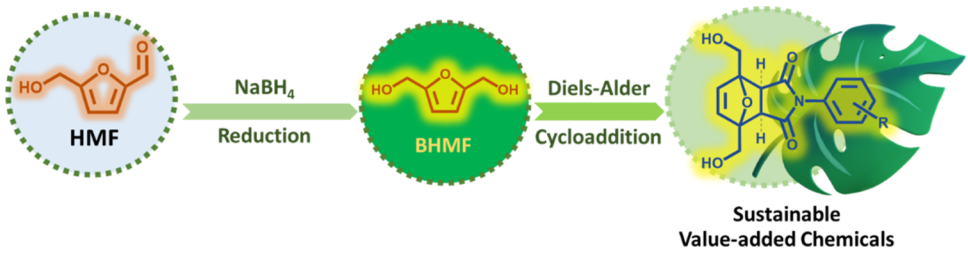

Figure 1. Schematic diagram of 5-HMF and its transformation into value-added chemicals.

poses several specific challenges that have limited its broader utilization.

The key limitation is the low reactivity of BHMF in typical Diels–Alder cycloadditions due to the aromatic character of its furan ring, which must be temporarily disrupted for the reaction to proceed.[26] As a result, harsh conditions involving high temperatures and catalytic Lewis or Brønsted acids are usually required to activate the furan toward cycloaddition.[29,30] These forcing conditions unfortunately promote several undesirable side reactions of the aldehyde moiety such as self-condensation and polymerization.[31−33] Competing polymerization, in particular, has proven difficult to avoid and greatly complicates the isolation and purification of Diels–Alder cycloadducts derived from BHMF.

More recent work has explored the use of substituted furan to enhance reactivity and selectivity in Diels–Alder cycloadditions, but even these substrates often suffer from poor atom economy due to the need for activating group installation and postreaction removal.[34] Selectivity issues also remain with substituted furan since both furan double bonds may be reactive, leading to uncontrolled regio- and stereoisomer formation.[35−39] Overcoming the challenges of side reactions and selectivity issues associated specifically with using biomass-derived substituted furan as a substrate therefore remains an active area of investigation for expanding the utility of Diels–Alder cycloadditions in renewable synthesis.[27,40−43]

Maleimides represent an interesting class of monomers for polymer synthesis due to their high reactivity in Diels–Alder reactions with furans.[26,44−47] Maleimides are currently derived from petroleum-based feedstocks. However, it is possible to synthesize maleic acid from the oxidation of furfural, while aniline derivatives can be synthesized from lignin.[48,49] As cyclic imides, maleimides exhibit exceptional thermal and chemical stability while also possessing versatile functionality that enables facile polymer modification.[27,50−52] Recent investigations have revealed the promising potential of maleimide-furan polymers as they can be synthesized under mild conditions and display superior mechanical properties, durability, and processability compared to traditional petroleum-based materials.[53−55] Additionally, the incorporation of maleimides introduces new topology into the polymer backbone, which directly translates into enhancements in thermal resistance, strength, and toughness.[56]

Moreover, maleimide-furan adducts have a large application in biomedical engineering due to their chemical frameworks as well as the presence of functional groups provides opportunities to develop biobased materials with specific characteristics,[57−60] for example, stimulus-responsive drug delivery systems and development of prodrugs.[61,62] Additionally, the maleimide-furan adducts are also modified for fluorescence sensor applications,[63−65] incorporation onto the surface of materials,[66] and the modification of properties of metal–organic frameworks[67−69] due to their flexible backbone structure. By varying the kinds of maleimides and furans that are incorporated into the formation of these adducts, the new materials can be designed to possess different properties, such as improved service life and elasticity.

Therefore, the use of renewable furanic rings coupled with reactive and stable maleimide monomers serves as an innovative platform for constructing high-performance sustainable polymers via Diels–Alder chemistry. In this work, we demonstrate the versatile reactivity and utility of maleimides as alternative monomers capable of producing tailor-made advanced materials.

EXPERIMENTAL SECTION

Chemicals. 1-(4-Hydroxyphenyl)-1*H*-pyrrole-2,5-dione (>98%), *N*-phenylmaleimide (>98%), *N*-(4-nitrophenyl)-maleimide (>98%), and 5-hydroxymethyl-2-furaldehyde stabilized with water (>95%) were purchased from Tokyo Chemical Industry Co. Ltd. (Tokyo, Japan). Aluminum thin-layer chromatography (TLC) plates coated with silica gel 60 F_{254} and anhydrous sodium sulfate were obtained from Sigma-Aldrich (Germany). Molecular sieves 4 Å (8 to 12 mesh) and sodium borohydride (98%) were obtained from Acros Organics. Phosphomolybdic acid (PMA) and toluene (99.5%) were rendered by Carlo Erba Reagents (Italy). Methanol (MeOH, 99.9%), ethyl acetate (EtOAc, 99.9%), dichloromethane (DCM, 99.9%), *n*-hexane (99.9%), tetrahydrofuran (THF, 99.9%), and acetone (99.9%) were purchased from Honeywell Chemicals. Ethanol (99.5%) and 1,4-dioxane (>99%) were ordered from Sigma-Aldrich (Germany). Acetonitrile (ACN, 99.8%, Sigma-Aldrich) was dried and stored over 4 Å molecular sieves. Chloroform (AR grade) and diethyl ether (AR grade) were delivered by RCI Labscan Limited (Germany). All solvents mentioned above were used as received unless otherwise stated.

Instrumentation. Nuclear magnetic resonance characterizations (^{1}H NMR, ^{13}C NMR) were carried out using a 400 MHz Bruker spectrometer. Products were dissolved in D_2O (Cambridge Isotope Laboratories), and DMSO-d_6 (Sigma-Aldrich) accordingly. The sample mixture was moved into 5 mm NMR tubes (16 scans at around 22 °C). Mass spectrum analysis involved the use of a Bruker Daltonics Compact high-resolution quadrupole time-of-flight (QTOF) instrument. Positive ionization polarity was considered. The single-crystal X-ray diffraction pattern was attained with the help of a Bruker D8 Quest diffractometer with a microfocus Cu X-ray source and a variable temperature control unit (100−400 K). Infrared spectra were recorded using a PerkinElmer modal Frontier spectrometer using the KBr pellet method between 400 and 4000 cm^{-1}. CHN elemental analysis was conducted via a Thermo Scientific FLASH 2000 series CHNS/O Analyzer.

https://doi.org/10.1021/acsomega.4c03804
ACS Omega 2024, 9, 36380−36388

Synthesis of 2,5-Di(hydroxymethyl)furan (BHMF). BHMF was synthesized using a method, slightly modified from the previous work by Kucherov et al.[70] In a 100 cm^3 round-bottom flask with a magnetic stirring bar, HMF (5 g, 40 mmol) was added in 70 cm^3 distilled water. Sodium borohydride (1.5 g, 40 mmol) was then dissolved in 15 cm^3 cooled deionized water, as dissolving it in water at room temperature reduces the yield since hydrogen gas evolves quickly before going into the reaction mixture. The sodium borohydride solution was added dropwise with constant stirring. The mixture was further stirred for 1 h at 24 °C. The reaction mixture was extracted using ethyl acetate (4 × 20 cm^3). After organic phases were collected, the liquid mixture was dried with anhydrous sodium sulfate before evaporating the solvent under a vacuum. Furthermore, it was recrystallized using dichloromethane, after vacuum filtration, and crystals were washed with cold diethyl ether. **^{1}H NMR (400 MHz, D_2O):** R_f value (EtOAc/*n*-hexane, 8:2): 0.59; δ (ppm) = 4.40 (s, 4H), 6.20 (s, 2H); **^{13}C NMR (400 MHz, D_2O):** δ (ppm) = 55.79, 109.06, 153.61; ESI-MS: *m*/*z* calculated for $[M]^+$ ($C_6H_8O_3$): 128.04734; found: 128.

General Synthesis of 4,7-Bis(hydroxymethyl)-2-(4-hydroxyphenyl)-3a,4,7,7a-tetrahydro-1H-4,7-epoxyisoindole-1,3(2H)-dione. In a 50 cm^3 round-bottom flask with a magnetic stirring bar, 1-(4-hydroxyphenyl)-1*H*-pyrrole-2,5-dione (505.1 mg, 2.67 mmol) and 2,5-di(hydroxymethyl)furan (BHMF) (372.9 mg, 2.91 mmol) were dissolved in 1.00 cm^3 acetonitrile under constant stirring. The mixture was stirred at the indicated temperature (Table 1) for 24 h under a reflux condition and then monitored by TLC demonstration to confirm the presence of the product. After the solvent was evaporated under reduced pressure, the collected dried product was purified by column chromatography (dry loading), using a solvent system (EtOAc/*n*-hexane, 8:2). The solvent removal from the collected fraction was carried out to obtain a white solid product (651.8 mg, 71%). Recrystallization was further performed using a binary solvent system with acetone and *n*-hexane.

Table 1. Optimization Study for the Diels−Alder Cycloaddition of BHMF (1) with *N*-(4-Hydroxyphenyl)maleimide (2A)

entry	solvent	time (h)	temperature (°C)	*endo*/*exo* ratio	yield (%)
1[a]	ACN	24	45	94:6	71.0
2[b]	acetone	24	55	67:33	41.0
3[b]	EtOAc	24	45	76:24	54.9
4[b]	toluene	24	80	86:14	3.0
5[b]	DCM	24	45	85:15	51.4
6[b]	*n*-hexane	24	45	96:4	13.3
7[a]	ACN	24	24	99:1	70.2
8[a]	MeOH	24	45	88:12	46.3
9[a]	ACN	24	70	54:46	18.8
10[a]	ACN	24	100	48:52	34.6
11[a]	ACN	24	120	67:33	33.0

[a]Ratio of BHMF and *N*-(4-hydroxyphenyl)maleimide is 1.09:1. [b]Ratio of BHMF and *N*-(4-hydroxyphenyl)maleimide is 1:1.[46,47]

*4,7-Bis(hydroxymethyl)-2-(4-hydroxyphenyl)-3a,4,7,7a-tetrahydro-1H-4,7-epoxyisoindole-1,3(2H)-dione (**3A**).* ^{1}H NMR (400 MHz, D_2O): R_f (EtOAc/*n*-hexane, 8:2) = 0.22; δ (ppm) = 3.67 (d, *J* = 4 Hz, 2H), 4.08 (dd, *J* = 52.9, 13.3 Hz, 4H), 6.50 (d, *J* = 4 Hz, 2H), 6.85 (dd, *J* = 16, 8 Hz, 4H); ^{13}C NMR (400 MHz, D_2O): δ (ppm) = 47.71, 59.82, 92.40, 116.44, 122.70, 128.32, 136.05, 156.72, 177.34; ESI-MS: *m*/*z* calculated for $[M + Na]^+$ ($C_{16}H_{15}NO_6$): 340.07916. Found: 340.0789; analytical elemental analysis data calculated for ($C_{16}N_{15}NO_6$): C, 60.57; H, 4.77; N, 4.41. Found: C, 59.78; H, 4.49; N, 4.24.

General Synthesis of 4,7-Bis(hydroxymethyl)-2-phenyl-3a,4,7,7a-tetrahydro-1H-4,7-epoxyisoindole-1,3(2H)-dione. In a 10 cm^3 round-bottom flask with a magnetic stirring bar, *N*-phenylmaleimide (135.1 mg, 0.78 mmol) and 2,5-di-(hydroxymethyl)furan (BHMF) (100 mg, 0.78 mmol) were dissolved in 1.686 cm^3 methanol under constant stirring. The reaction mixture was stirred at the indicated temperature (Table 2) for 24 h, and then monitored by TLC demonstration to confirm the formation of the product. After the solvent was evaporated under reduced pressure, the dried product was then dissolved in DCM, and the collected dried product was purified by column chromatography (dry loading), using a solvent system (EtOAc/*n*-hexane, 8:2). The solvent removal from the collected fraction was carried out to obtain a white solid product (195.2 mg, 83%). Recrystallization was carried out under a binary solvent system with acetone and *n*-hexane.

Table 2. Optimization Study for the Diels−Alder Cycloaddition of BHMF (1) with *N*-Phenylmaleimide (2B)

entry	solvent	time (h)	temperature (°C)	*endo*/*exo* ratio	yield (%)
1[a]	ACN	24	45	13:87	18.6
2[a]	diethyl ether	24	40	24:76	22.7
3[a]	MeOH	24	45	38:62	68.1
4[a]	EtOAc	24	45	10:90	52.7
5[a]	*n*-hexane	24	45	1:99	22.8
6[a]	MeOH	24	24	5:95	83.0
7[a]	MeOH	24	70	34:66	40.1
8[b]	EtOAc	24	45	1:99	37.2
9[b]	DCM	24	rt	0:100	27.9
10[b]	1,4-dioxane	24	rt	1:99	45.5
11[c]	DCM	24	45	25:75	50.9
12[c]	EtOAc	24	45	0:100	45.6

[a]Ratio of BHMF to *N*-phenylmaleimide is 1.0:1.0. [b]Ratio of BHMF to *N*-phenylmaleimide is 1.0:1.52. [c]Ratio of BHMF and *N*-(phenyl)maleimide is 0.92.[26,28,46,47]

*4,7-Bis(hydroxymethyl)-2-phenyl-3a,4,7,7a-tetrahydro-1H-4,7-epoxyisoindole-1,3(2H)-dione (**4B**).* ^{1}H NMR (400 MHz, D_2O): R_f (EtOAc/*n*-hexane, 8:2) = 0.28; δ (ppm) = 3.72 (s, 2H) 4.09 (dd, *J* = 52, 12 Hz, 4H), 6.52 (s, 2H), 7.02 (dd, *J* = 8, 4 Hz, 2H), 7.38−7.42 (m, 3H); ^{13}C NMR (400 MHz, D_2O): δ (ppm) = 47.85, 59.82, 92.44, 126.78, 129.84, 129.99, 130.49, 136.10, 177.02; ESI-MS: *m*/*z* calculated for $[M + Na]^+$ ($C_{16}H_{15}NO_5$): 324.08424. Found: 324.0837; analytical elemental analysis data calculated for ($C_{16}H_{15}NO_5$): C, 63.78; H, 5.02; N, 4.65. Found: C, 64.15; H, 4.95; N, 3.51.

General Synthesis of 4,7-Bis(hydroxymethyl)-2-(4-nitrophenyl)-3a,4,7,7a-tetrahydro-1H-4,7-epoxyisoindole-1,3(2H)-dione. In a 10 cm^3 round-bottom flask with a magnetic stirring bar, *N*-(4-nitrophenyl)maleimide (153.3 mg, 0.70 mmol) and 2,5-di(hydroxymethyl)furan (BHMF) (90 mg, 0.70 mmol) were dissolved in 3 cm^3 ethyl acetate under constant stirring. The reaction mixture was stirred at the indicated temperature (Table 3) for 24 h and then monitored

https://doi.org/10.1021/acsomega.4c03804
ACS Omega 2024, 9, 36380−36388

Table 3. Optimization Study for Diels–Alder Cycloaddition of BHMF (1) with *N*-(4-Nitrophenyl)maleimide (2C)

entry	solvent	time (h)	temperature (°C)	*endo*/*exo* ratio	yield (%)
1[a]	ACN	24	40	98:2	25.9
2[b]	EtOAc	24	45	86:14	92.5
3[b]	*n*-hexane	24	50	89:11	20.1
4[b]	EtOAc	24	24	92:8	90.2
5[b]	MeOH	24	45	88:12	36.8
6[b]	EtOAc	24	70	8:92	74.1

[a]Ratio of BHMF, *N*-(4-nitrophenyl)maleimide is 1.22:1. [b]Ratio of BHMF, *N*-(4-nitrophenyl)maleimide is 1:1.[39,46]

by TLC demonstration to confirm the formation of the product. After the solvent was evaporated under reduced pressure, the dried product was then dissolved in DCM, and the collected dried product was purified by column chromatography (dry loading), using a solvent system (EtOAc/*n*-hexane, 8:2). The solvent removal from the collected fraction was carried out to obtain a white solid product (224.3 mg, 92.5%). Recrystallization was carried out under a binary solvent system using ACN and *n*-hexane.

*4,7-Bis(hydroxymethyl)-2-(4-nitrophenyl)-3a,4,7,7a-tetrahydro-1H-4,7-epoxyisoindole-1,3(2H)-dione (**3C**).* ^{1}H NMR (400 MHz, DMSO-d_6): R_f (EtOAc/*n*-hexane, 8:2) = 0.24; δ (ppm) = 3.71 (s, 2H), 3.98 (ddd, J = 31.6, 12.6, 6.2 Hz, 4H), 5.24 (t, J = 5.7 Hz, 2H, OH), 6.51 (s, 2H), 7.47 (d, J = 8 Hz, 2H), 8.32 (d, J = 8 Hz, 2H); ^{13}C NMR (400 MHz, DMSO-d_6): δ (ppm) = 47.52, 59.62, 92.67, 124.26, 127.80, 136.23, 137.46, 146.69, 173.88; ESI-MS: m/z calculated for $[M + Na]^+$ ($C_{16}H_{14}N_2O_7$): 369.06932. Found: 369.0692; analytical elemental analysis data calculated for ($C_{16}H_{14}N_2O_7$)·H_2O: C, 52.75; H, 4.43; N, 7.69. Found: C, 53.73; H, 3.73; N, 7.60.

*4,7-Bis(hydroxymethyl)-2-(4-nitrophenyl)-3a,4,7,7a-tetrahydro-1H-4,7-epoxyisoindole-1,3(2H)-dione (**4C**).* ^{1}H NMR (400 MHz, DMSO-d_6): R_f (EtOAc/*n*-hexane, 8:2) = 0.22; δ (ppm) = 3.20 (*s*, 2H), 3.93 (ddd, J = 118.8, 12.4, 5.6 Hz, 4H), 5.03 (t, J = 5.64 Hz, 2H, OH), 6.57 (s, 2H), 7.55 (d, J = 8 Hz, 2H), 8.35 (d, J = 8 Hz, 2H); ^{13}C NMR (400 MHz, DMSO-d_6): δ (ppm) = 51.04, 59.06, 91.85, 124.32, 127.71, 137.58, 138.32, 146.59, 173.42. Analytical elemental analysis data were calculated for ($C_{16}H_{14}N_2O_7$)·CH_3OH: C, 53.97; H, 4.80; N, 7.40. Found: C, 54.14; H, 3.90; N, 7.40.

Computation Details. All calculations were carried out using Gaussian 09.[71] In this work, two functionals have been used, namely, the density functional B3LYP with a 6-31g(d) basis set and the M06-2X functional with a 6-311++g(d,p) basis set. Pertaining to the less torsion angle distortion between the phenyl and maleimide rings from the actual bond angle values in all three products, M06-2*X*/6-311++g(d,p) shows better attributes than B3LYP/6-31g(d). In addition, the former renders much better energy consideration for Diels–Alder cycloaddition and has been widely considered.

RESULTS AND DISCUSSION

BHMF was yielded from the reduction of HMF by $NaBH_4$ and was characterized by ^{1}H NMR, ^{13}C NMR, and ESI-MS (see Figures S1–S3). The reaction of BHMF with *N*-phenylmaleimide derivatives using optimal conditions gave the Diels–Alder products, **3A**, **4B**, **3C**, and **4C**. The analytical and spectral data of four new compounds were the tools of structural elucidation (see Figures S4–S40). BHMF reacted with *N*-(4-hydroxyphenyl)maleimide to give *N*-(hydroxyphenyl)-derivative **3A**. To confirm NMR spectroscopic data of compound **3A** (*endo* isomer), the peak at 3.67 ppm (d, J = 4 Hz, 2H) corresponds to the bridging protons between a maleimide ring and BHMF, four protons on the hydroxymethyl arm on either side of the adduct are shown at 4.08 ppm (dd, J = 52.9, 13.3 Hz, 4H), and the peaks at 6.50 ppm (d, J = 4 Hz, 2H) and 6.85 ppm (dd, J = 16, 8 Hz, 4H) correspond to four aromatic protons at *ortho* and *meta* positions of the phenyl ring and protons of the unsaturated bicyclic ring (see Figure S4). Considering the structure of compound **4B** (*exo* isomer), BHMF reacted with *N*-phenylmaleimide; likewise, the singlet of the bridging proton was obtained at 3.72 ppm (s, 2H), five protons of phenyl ring appeared at 7.02 ppm (dd, J = 8, 4 Hz, 2H) and 7.38–7.42 ppm (m, 3H), protons of two methine carbons in the bicyclic ring assessed at 6.52 ppm (s, 2H), and the peak at 4.09 ppm (dd, J = 52, 12 Hz, 4H) marked the methylene protons (see Figure S14). The reaction of BHMF with *N*-(4-nitrophenyl)maleimide gave two isolated compounds, **3C** and **4C**. For *endo* isomer (**3C**), the single peak at 3.71 ppm corresponded to bridging protons, and the peak at 3.98 ppm (ddd, J = 31.6, 12.6, 6.2 Hz, 4H) depicted the CH_2 protons close to the methine protons 6.51 ppm (s, 2H) (see Figure S24). For compound **4C** (*exo* isomer), a singlet of the bridge proton was calibrated at 3.20 ppm (s, 2H) (see Figure S34). From the spectrum of compound **3C**, the triplet peak due to the hydroxy group appeared at 5.24 ppm (t, J = 5.7 Hz, 2H, OH); however, it showed up at 5.03 ppm (t, J = 5.64 Hz, 2H, OH) in compound **4C**.

Next, ^{13}C NMR spectroscopy was performed to confirm the structures of the synthesized compounds. In compound **3A**, the carbonyl peak was observed at 177.34 ppm; meanwhile, the predicted value was 173.3 ppm, and the signal attributed to the furan maleimide bridge was observed at 47.71 ppm (see Figure S6). For compound **4B**, 47.85 ppm was assigned to the signal of maleimide carbon joining with the furanic ring (see Figure S16). For compounds **3C** and **4C**, signals at 47.52 and 51.04 ppm were attributed to bridging carbons linked with BHMF, respectively (see Figures S26 and S35). Moreover, DEPT-90, DEPT-135, ^{1}H–^{1}H COSY, ^{1}H–^{13}C HSQC, and ^{1}H–^{13}C HMBC spectroscopic data of newly proposed compounds were further investigated and presented in this work for the first time (see the Supporting Information).

In this work, the infrared spectral data of newly synthesized compounds were studied successfully. The IR spectrum of compound **3A** showed a characteristic sharp aliphatic –OH stretching frequency at 3432 cm^{-1}, and the C(sp^2)–H aromatic stretching frequency was slightly higher than the alkyl C(sp^2)–H, with the former showing in the range of 3064–3082 cm^{-1} and the latter in the range of 2851–2917 cm^{-1} (see Figure S12). Compound **4B** showed a much broader and lower –OH bond stretching frequency (3255 cm^{-1}) among all three cases due to extensive hydrogen bonding (see Figure S22). For compound **3C**, the stretching frequency (3417 cm^{-1}) was almost comparable to that of **3A** (see Figure S32).

Next, mass spectrometry (MS) is a very flexible and comprehensive analytical method that is examined to confirm the molar mass of the obtained synthesized compounds. The m/z ratios of their molecular ions correspond precisely to the predicted accurate masses, indicating the stability of these ions (Figures S3, S13, S23, and S33). The aforementioned results of NMR spectra and mass analytical examinations confirm the

https://doi.org/10.1021/acsomega.4c03804
ACS Omega 2024, 9, 36380–36388

successful synthesis of the proposed compounds. The elemental analysis of the products obtained from the Diels–Alder process closely matched the expected structure.

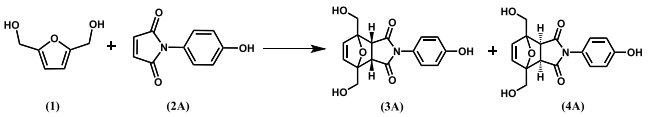

The investigation commenced by employing 2,5-di-(hydroxymethyl)furan (BHMF) (**1**) in chemical transformation with *N*-(4-hydroxyphenyl)maleimide (**2A**) as the model reaction. This particular substrate has posed challenges in the earlier literature.[26] In our initial experiment, conducted at a temperature of 80 °C under controlled conditions and with equal amounts of reactants, we obtained an approximate amount of the desired product (3% yield) with a ratio of 86:14 between the *endo* and *exo* isomers (Table 1, entry 4). By increasing the ratio of reagents to 1.09:1 (BHMF/*N*-(4-hydroxyphenyl)maleimide), a favorable outcome was observed as the yield of the corresponding product reached 71% (Table 1, entry 1). Subsequently, we performed the reaction using various solvents, as indicated in Table 1 (entries 2–3, 5–8). Recognizing the necessity for environmentally friendly chemistry research and our desire to prioritize sustainability, we redirected our focus toward solvent consumption that is classified as "cost-effective" by the chemical process. Using acetonitrile resulted in a 70% yield with a considerable preference for the endo product (Table 1, entry 7). The highest results were achieved with around a 71% yield and a 99% *endo*-isomer selectivity when acetonitrile was employed as the solvent (Table 1, entry 7). This solvent allowed for lower reaction temperatures. When acetonitrile was used as a solvent, increasing the reaction temperature resulted in a decrease in the reaction yield (Table 1, entries 2, 9–11). The investigation of the screening of solvents on yield was carried out. Polar solvents, particularly acetonitrile and methanol, improved yields because hydrogen bonding stabilized the transition state. Nonpolar solvents like toluene, diethyl ether, and *n*-hexane resulted in significantly lower yields compared to those of polar solvents.

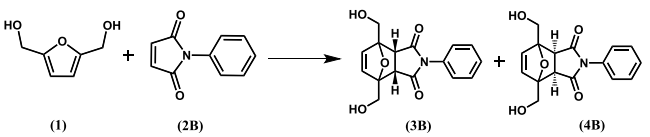

We discovered a shift in selectivity in the reaction of BHMF and *N*-(phenyl)maleimide while studying the identical reaction at room temperature, as shown in Table 2. Generally, at a higher temperature, the thermodynamic *exo* product is preferred, whereas, at normal temperature, the kinetic endo product is more readily produced. The diastereoselectivity of furan Diels–Alder cycloadditions is governed by either thermodynamic or kinetic control principles. The thermodynamic regulation of a reaction system states that when there is an increase in heat and energy, the formation of a more thermodynamically stable product is favored. The *exo* one product is more stable due to reduced steric hindrance when the oxygen-atom bridge is positioned on the same side as the maleimide ring substituent. However, the *endo* product is kinetically favored (kinetic control) and is more easily formed. This is because a secondary interaction is expected to occur between the electron-deficient carbonyl groups of the dienophile and the emerging π bond at the back of the diene. As a result, the energy of the transition state barrier is reduced.[72] When transitioning from theory to application, it becomes obvious that thermodynamic control is more dominant at higher temperatures, but at room temperature, the *endo* product is predominantly generated. Regrettably, the proportion of the endo adduct for *N*-phenylmaleimide in all solvents was consistently low, as indicated in Table 2. The highest yield of 83% with a selectivity of 95% toward the desired product was achieved when methanol (MeOH) was used as the solvent, as shown in Table 2, entry 11. Regardless of the situation, the crude reaction mixture primarily contains only the product and starting materials. Starting materials remain unchanged if they have not undergone a reaction, allowing maleimide to be reused after it is separated from the crude reaction mixture.

Afterward, we proceeded to examine the range of substrates that can be used in the experiment conducted at room temperature, with a particular focus on the likelihood of observing a preference for endo products. Table 2, entry 6, shows that a 45% yield of the appropriate product was produced for the model substrate *N*-phenylmaleimide, with a 99% *exo* selectivity. In a separate reaction combination, conducted using dichloromethane (DCM), a 100% *exo* selectivity was achieved with a yield of 28% (Table 2, entry 5). Based on the information provided in Table 2, entries 4, 5, and 8, it can be inferred that manipulating the ratio of furanic diene has a substantial impact on promoting *exo* selectivity. By increasing the temperature, the yield of the product decreased by half, dropping from 83% at 24 °C to 40% at 70 °C. Additionally, the *endo*:*exo* ratio was increased, shifting from 5:95 to 34:66 (Table 2, entries 6 and 7).

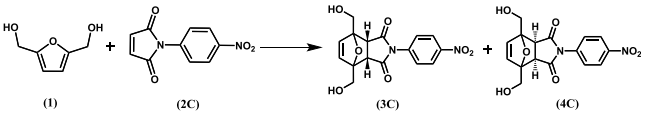

Next, we attempted the reaction of the *para*-nitro maleimide derivative with anhydrous ACN in a ratio of 1.22:1 (BHMF/*N*-(4-nitrophenyl)maleimide). The reaction exhibited *endo* selectivity, but the yield was still low, as shown in Table 3, entry 1. Additionally, throughout the experiment, when using a 1:1 ratio of BHMF to *N*-(4-nitrophenyl)maleimide in the presence of ethyl acetate (EtOAc), the yield was increased dramatically to 93% with an *endo*/*exo* ratio of 86:14 (Table 3, entry 2). The addition of MeOH (Table 3, entry 5) resulted in a decrease in the yield to 37% and an *endo*/*exo* ratio of 88:12. Using *N*-(4-nitrophenyl)maleimide as a costarting material, experimental results showed a different trend compared to the previous two maleimide derivatives. It demonstrates a high degree of thermodynamic and kinetic control that is extremely predictable (Table 3, entries 1–6). As was to be predicted, the reaction that was carried out at 70 °C produced an *exo* selectivity adduct in a yield of 74%. This explains why increasing the temperature further pushes the reaction in the opposite way by driving the retro Diels–Alder reaction, which is described in Table 3, entry 6. Only 20% of the equivalent product was obtained when *n*-hexane was used as the solvent, even though the *endo*/*exo* ratio was 89:11. When EtOAc was used at 45 °C, the highest yield of 92% was achieved (entry 2). On the other hand, we were not successful in separating the *endo* and *exo* pure products since, when monitored with TLC, they exhibited a small difference between R_f values of just 0.02.

https://doi.org/10.1021/acsomega.4c03804
ACS Omega 2024, 9, 36380–36388

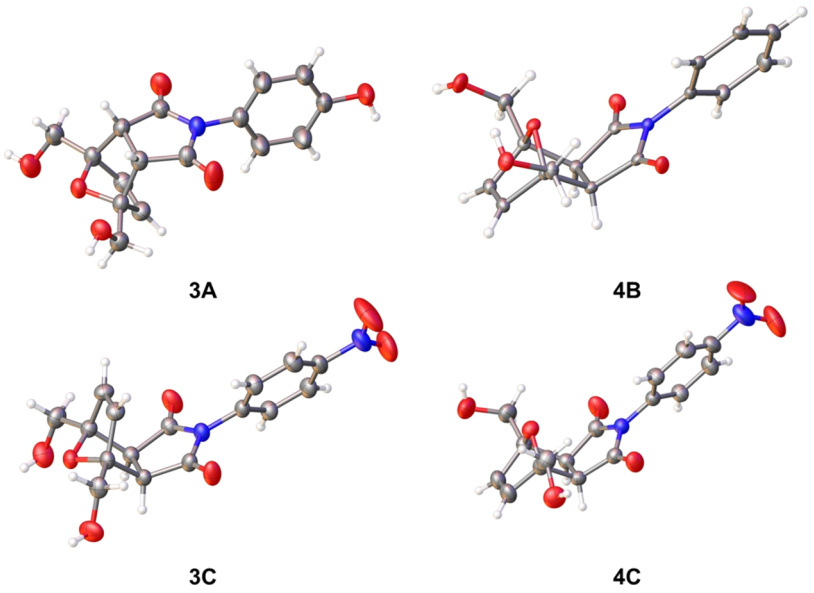

Figure 2. Crystal structures of compounds **3A**, **4B**, **3C**, and **4C** determined from single-crsytal X-ray diffraction experiments. Atoms are plotted as thermal ellipsoids at the 50% probability level. Gray, red, and blue ellipsoids and white spheres represent carbon, oxygen, nitrogen, and hydrogen atoms, respectively. A cocrystallized solvent molecule in **3C** and a disordered component in **4C** are omitted for clarity.

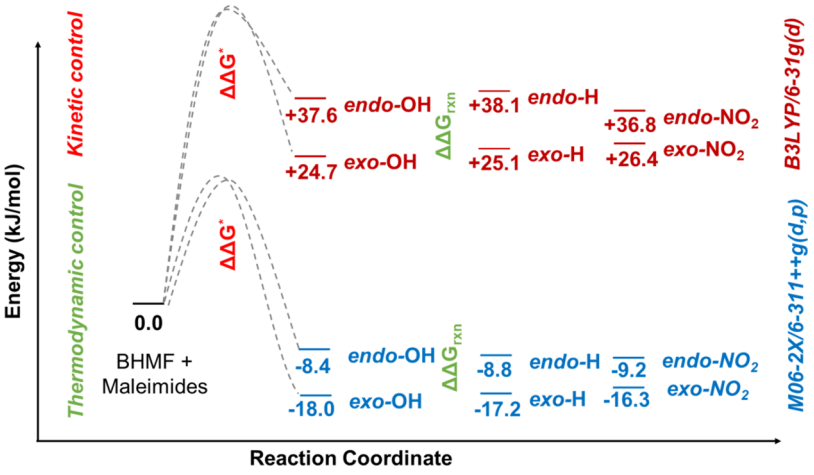

Figure 3. Free energy profile for the transformation of BHMF and *N*-phenylmaleimide derivatives.

An electron-rich diene and an electron-poor dienophile are the two components that are involved in the Diels−Alder reaction. This reaction is characterized by the interaction between the highest occupied molecular orbital (HOMO) of the diene and the lowest unoccupied molecular orbital (LUMO) of the dienophile. In the event that the electrical characteristics or energy levels of the orbitals are incompatible with one another, it is possible that the reaction will not proceed.

The crystal structures of the novel synthesized compounds were determined by X-ray diffraction, and crystal structures are shown in Figure 2. From obtained analytical data (see Tables S1−S13), to begin with, the bond length between maleimide's nitrogen atom and the phenyl ring increases by an iota of difference from 1.428(2), 1.433(2), and 1.438(2) to 1.441(2) Å for **4C**, **3C**, **4B**, and **3A**. This is probably due to the partial double bond character, which becomes more prominent going from a hydroxy substituent (for **3A**) to a nitro substituent (for **3C** and **4C**) due to its electron-withdrawing nature, making the phenyl ring increasingly electron deficient. Furthermore, in the nitro derivative, the new C···C bonds formed between furanic and maleimide rings are, on average, longer in compound **4C** than in **3C**, **3A**, and **4B** (Table S1, entries 5 and 6).

Density functional theory (DFT) calculations were used to explain the selectivity of the *endo* and *exo* products. All six novel structures were optimized with converged frequencies, as lower-energy products tend to form easily and are determined for the lowest energy, considering their higher stability (Figure 3). The first optimization was carried out at the B3LYP/6-31g(d) level. However, due to the large torsion angle value error between the phenyl ring and maleimide nitrogen in the crystal value and the computationally optimized geometries, the M06-2*X*/6-311++g(d,p) level was used instead. Based on computational results, it is obvious that the structures of *exo* isomers are more thermodynamically stable than those of *endo* isomers, as computationally favored forms had more negative energy in all cases, which is consistent with the previous literature.[73,74] For the switching of isomers of major products, increasing the temperature caused the reaction to occur at **4C**, showing the narrowest energy difference between **3C** and **4C**

https://doi.org/10.1021/acsomega.4c03804
ACS Omega 2024, 9, 36380−36388

at 7.1 kJ/mol, while the other products from *N*-phenylmaleimide (**3B** and **4B**) and *N*-(4-hydroxyphenyl)maleimide (**3A** and **4A**) showed an energy difference of 8.4 and 9.6 kJ/mol, respectively.

In summary, our method for the Diels−Alder cycloaddition of BHMF and *N*-phenylmaleimide derivatives has the capacity to provide possibilities for several upcoming applications. Furthermore, the method is not only moderate and easy to use, but it is also well-suited for expansion and growth. We had success in enhancing the yield of all three products, resulting in a favorable conclusion.

CONCLUSIONS

In summary, this study focuses on the transformation of traditional biomass into a new compound using the Diels−Alder cycloaddition process. We attempted to elucidate the influence of solvent, temperature, and equivalent ratio on the optimization of the reaction. All new compounds have been established in acceptable yields and successfully characterized by essential techniques, including one-dimensional (1D) NMR spectroscopy (^{1}H, ^{13}C, DEPT-90, and DEPT- 135), two-dimensional (2D) NMR spectroscopy (^{1}H−^{1}H COSY, ^{1}H−^{13}C HSQC, and ^{1}H−^{13}C HMBC), IR, elemental analysis, mass spectrum (QTOF), and single-crystal X-ray diffraction (SC-XRD), and supported the theoretical properties by DFT calculation methods. Furthermore, this research emphasizes the importance of sustainable synthetic techniques and provides vital insights into the advancement of environmentally friendly, new avenues as the tunable precursor for challenging functionalized polymers in the future.

ASSOCIATED CONTENT

Supporting Information

The Supporting Information is available free of charge at https://pubs.acs.org/doi/10.1021/acsomega.4c03804.

Details about X-ray crystallographic analytical results, NMR spectra, mass spectra, and IR spectra of products (PDF)

ES003_0ma (CIF)

ES005_0ma (CIF)

ES006_0ma (CIF)

ES003_0ma (CIF)

AUTHOR INFORMATION

Corresponding Author

Ekasith Somsook − *NANOCAST Laboratory, Center for Catalysis Science and Technology (CAST), Department of Chemistry and Center of Excellence for Innovation in Chemistry, Faculty of Science, Mahidol University, Ratchathewi, Bangkok 10400, Thailand;* orcid.org/0000-0002-4659-8349; Phone: +66-2-201-5123; Email: ekasith.som@mahidol.ac.th

Authors

Harshit Shukla − *NANOCAST Laboratory, Center for Catalysis Science and Technology (CAST), Department of Chemistry and Center of Excellence for Innovation in Chemistry, Faculty of Science, Mahidol University, Ratchathewi, Bangkok 10400, Thailand*

Peerapong Promcharoen − *NANOCAST Laboratory, Center for Catalysis Science and Technology (CAST), Department of Chemistry and Center of Excellence for Innovation in Chemistry, Faculty of Science, Mahidol University, Ratchathewi, Bangkok 10400, Thailand*

Thinnaphat Poonsawat − *NANOCAST Laboratory, Center for Catalysis Science and Technology (CAST), Department of Chemistry and Center of Excellence for Innovation in Chemistry, Faculty of Science, Mahidol University, Ratchathewi, Bangkok 10400, Thailand*

Khetpakorn Chakarawet − *Department of Chemistry, Faculty of Science, Mahidol University, Ratchathewi, Bangkok 10400, Thailand;* orcid.org/0000-0001-5905-3578

Peerapong Chumkaeo − *NANOCAST Laboratory, Center for Catalysis Science and Technology (CAST), Department of Chemistry and Center of Excellence for Innovation in Chemistry, Faculty of Science, Mahidol University, Ratchathewi, Bangkok 10400, Thailand*

Complete contact information is available at: https://pubs.acs.org/10.1021/acsomega.4c03804

Author Contributions

H.S. contributed to conceptualization, methodology, investigation, validation, visualization, and writing—original draft. P.P. and T.P. contributed to investigation and recommendation. K.C. contributed to crystal structure analysis. P.C. contributed to research design, data analysis, conclusion, recommendation, writing—reviewing and editing, and supervision. E.S. contributed to conventionalization, investigation, writing—original draft, supervision, and project administration.

Notes

The authors declare no competing financial interest.

ACKNOWLEDGMENTS

This research was supported by the NSRF *via* the Program Management Unit for Human Resources & Institutional Development, Research, and Innovation [Grant No. B16F640099] and a research grant from the Center of Excellence for Innovation in Chemistry (PERCH−CIC) and the Center of Excellence in Petrochemical and Materials Technology (PETROMAT), Ministry of Higher Education, Science, Research, and Innovation (PERCH-CIC/RG-2565-01). T.P. would like to thank the Development and Promotion of Science and Technology Talents Project (DPST) for his scholarship. P.C. would like to thank Mahidol University for the postdoctoral fellowship. The authors thank Amporn Saekee for assistance in crystallographic data collection. They also thank the Faculty of Science, Mahidol University, for the use of the X-ray diffractometer.

REFERENCES

(1) Zhang, T.; Li, W.; Xiao, H.; Jin, Y.; Wu, S. Recent progress in direct production of furfural from lignocellulosic residues and hemicellulose. *Bioresour. Technol.* **2022**, *354*, No. 127126.

(2) Cañada-Barcala, A.; Rodríguez-Llorente, D.; López, L.; Navarro, P.; Hernández, E.; Águeda, V. I.; Álvarez-Torrellas, S.; Parajó, J. C.; Rivas, S.; Larriba, M. Sustainable Production of Furfural in Biphasic Reactors Using Terpenoids and Hydrophobic Eutectic Solvents. *ACS Sustainable Chem. Eng.* **2021**, *9* (30), 10266−10275.

(3) Naga Sai, M. S.; De, D.; Satyavathi, B. Sustainable production and purification of furfural from waste agricultural residue: An insight into integrated biorefinery. *J. Cleaner Prod.* **2021**, *327*, No. 129467.

(4) Wang, Z.; Xia, S.; Wang, X.; Fan, Y.; Zhao, K.; Wang, S.; Zhao, Z.; Zheng, A. Catalytic production of 5-hydroxymethylfurfural from lignocellulosic biomass: Recent advances, challenges and opportunities. *Renewable Sustainable Energy Rev.* **2024**, *196*, No. 114332.

(5) Yan, P.; Wang, H.; Liao, Y.; Wang, C. Zeolite catalysts for the valorization of biomass into platform compounds and biochemicals/biofuels: A review. *Renewable Sustainable Energy Rev.* **2023**, *178*, No. 113219.
(6) Chang, H.; Bajaj, I.; Motagamwala, A. H.; Somasundaram, A.; Huber, G. W.; Maravelias, C. T.; Dumesic, J. A. Sustainable production of 5-hydroxymethyl furfural from glucose for process integration with high fructose corn syrup infrastructure. *Green Chem.* **2021**, *23* (9), 3277−3288.
(7) Castiello, C.; Junghanns, P.; Mergel, A.; Jacob, C.; Ducho, C.; Valente, S.; Rotili, D.; Fioravanti, R.; Zwergel, C.; Mai, A. GreenMedChem: the challenge in the next decade toward eco-friendly compounds and processes in drug design. *Green Chem.* **2023**, *25* (6), 2109−2169.
(8) Karnjanakom, S.; Bayu, A.; Maneechakr, P.; Samart, C.; Kongparakul, S.; Guan, G. Rapid Transformation of Furfural to Biofuel Additive Ethyl Levulinate with In Situ Suppression of Humins Promoted by an Acidic-Oxygen Environment. *ACS Sustainable Chem. Eng.* **2021**, *9* (42), 14170−14179.
(9) Mittal, A.; Pilath, H. M.; Johnson, D. K. Direct Conversion of Biomass Carbohydrates to Platform Chemicals: 5-Hydroxymethylfurfural (HMF) and Furfural. *Energy Fuels* **2020**, *34* (3), 3284−3293.
(10) Nilaphai, O.; Thepwatee, S.; Kaeopookum, P.; Chuaitammakit, L. C.; Wongchaichon, C.; Rodjang, O.; Pudsong, P.; Singhapon, W.; Burerat, T.; Kamtaw, S.; et al. Synthesis of 5-(Hydroxymethyl)furfural Monoesters and Alcohols as Fuel Additives toward Their Performance and Combustion Characteristics in Compression Ignition Engines. *ACS Omega* **2023**, *8* (19), 17327−17336.
(11) Zhang, Y.; Jia, G.; Wang, W.; Jiang, L.; Guo, Z. Photocatalytic upgrading of 5-hydroxymethylfurfural − aerobic or anaerobic? *Green Chem.* **2024**, *26* (6), 2949−2966.
(12) Zhang, J.; Liu, B.; Zhou, Y.; Essawy, H.; Liang, J.; Zhou, X.; Du, G. Preparation and characterization of a bio-based rigid plastic based on gelatinized starch cross-linked with furfural and formaldehyde. *Ind. Crops Prod.* **2022**, *186*, No. 115246.
(13) Manjunathan, P.; Rao, B. S.; Lee, M.; Hidajat, M. J.; Yun, G.-N.; Hwang, D. W. Integrated process towards sustainable renewable plastics: Production of 2,5-furandicarboxylic acid from fructose in a base-free environment. *Appl. Catal., A* **2023**, *667*, No. 119446.
(14) Parmaki, S.; Vasquez, M. I.; Patsalou, M.; Gomes, R. F. A.; Simeonov, S. P.; Afonso, C. A. M.; Koutinas, M. Ecotoxicological assessment of biomass-derived furan platform chemicals using aquatic and terrestrial bioassays. *Environ. Sci.: Processes Impacts* **2024**, *26*, 686.
(15) Alonso-Fagúndez, N.; Granados, M. L.; Mariscal, R.; Ojeda, M. Selective Conversion of Furfural to Maleic Anhydride and Furan with VOx/Al2O3 Catalysts. *ChemSusChem* **2012**, *5* (10), 1984−1990.
(16) Tongtummachat, T.; Jaree, A.; Thongkan, K.; Chuphueak, W.; Akkarawatkhoosith, N. Continuous production of 5-hydroxymethylfurfural: A catalyst-free approach using non-toxic solvents for pharmaceutical applications. *Chem. Eng. J. Adv.* **2024**, *18*, No. 100597.
(17) Mariscal, R.; Maireles-Torres, P.; Ojeda, M.; Sádaba, I.; López Granados, M. Furfural: a renewable and versatile platform molecule for the synthesis of chemicals and fuels. *Energy Environ. Sci.* **2016**, *9* (4), 1144−1189.
(18) Bielski, R.; Grynkiewicz, G. Furan platform chemicals beyond fuels and plastics. *Green Chem.* **2021**, *23* (19), 7458−7487.
(19) Kong, Q.-S.; Li, X.-L.; Xu, H.-J.; Fu, Y. Conversion of 5-hydroxymethylfurfural to chemicals: A review of catalytic routes and product applications. *Fuel Process. Technol.* **2020**, *209*, No. 106528.
(20) Kucherov, F. A.; Romashov, L. V.; Galkin, K. I.; Ananikov, V. P. Chemical Transformations of Biomass-Derived C6-Furanic Platform Chemicals for Sustainable Energy Research, Materials Science, and Synthetic Building Blocks. *ACS Sustainable Chem. Eng.* **2018**, *6* (7), 8064−8092.
(21) Troiano, D.; Orsat, V.; Dumont, M.-J. Status of Biocatalysis in the Production of 2,5-Furandicarboxylic Acid. *ACS Catal.* **2020**, *10* (16), 9145−9169.
(22) Das, S.; Cibin, G.; Walton, R. I. Selective Oxidation of Biomass-Derived 5-Hydroxymethylfurfural Catalyzed by an Iron-Grafted Metal−Organic Framework with a Sustainably Sourced Ligand. *ACS Sustainable Chem. Eng.* **2024**, *12* (14), 5575−5585.
(23) Post, C.; Maniar, D.; Voet, V. S. D.; Folkersma, R.; Loos, K. Biobased 2,5-Bis(hydroxymethyl)furan as a Versatile Building Block for Sustainable Polymeric Materials. *ACS Omega* **2023**, *8* (10), 8991−9003.
(24) Tavana, J.; Faysal, A.; Vithanage, A.; Gramlich, W. M.; Schwartz, T. J. Pathway to fully-renewable biobased polyesters derived from HMF and phenols. *Polym. Chem.* **2022**, *13* (9), 1215−1227.
(25) Howell, B. A.; Lazar, S. T. Biobased Plasticizers from Carbohydrate-Derived 2,5-Bis(hydroxymethyl)furan. *Ind. Eng. Chem. Res.* **2019**, *58* (3), 1222−1228.
(26) Cioc, R. C.; Lutz, M.; Pidko, E. A.; Crockatt, M.; van der Waal, J. C.; Bruijnincx, P. C. A. Direct Diels−Alder reactions of furfural derivatives with maleimides. *Green Chem.* **2021**, *23* (1), 367−373.
(27) Cioc, R. C.; Harsevoort, E.; Lutz, M.; Bruijnincx, P. C. A. Efficient synthesis of fully renewable, furfural-derived building blocks via formal Diels−Alder cycloaddition of atypical addends. *Green Chem.* **2023**, *25* (23), 9689−9694.
(28) Cioc, R. C.; Smak, T. J.; Crockatt, M.; van der Waal, J. C.; Bruijnincx, P. C. A. Furoic acid and derivatives as atypical dienes in Diels−Alder reactions. *Green Chem.* **2021**, *23* (15), 5503−5510.
(29) van Scodeller, I.; De Oliveira Vigier, K.; Muller, E.; Ma, C.; Guégan, F.; Wischert, R.; Jérôme, F. A Combined Experimental−Theoretical Study on Diels-Alder Reaction with Bio-Based Furfural: Towards Renewable Aromatics. *ChemSusChem* **2021**, *14* (1), 313−323.
(30) Sun, S.; Fu, C.; Yu, X.; Yi, X.; Zheng, A.; Gu, Y.; Shi, H. On the reactivity and selectivity trends in the tandem Diels-Alder cycloaddition and dehydrative aromatization between dimethylfuran and ethene over solid acids. *J. Catal.* **2024**, *432*, No. 115418.
(31) Gancedo, J.; Faba, L.; Ordóñez, S. Tuning the selectivity on the furan-propylene Diels-Alder condensation over acid catalysts: Role of pore topology and surface acidity. *Appl. Catal., A* **2022**, *641*, No. 118683.
(32) Mikroyannidis, J. A. Synthesis and diels−alder polymerization of furfurylidene and furfuryl-substituted maleamic acids. *J. Polym. Sci., Part A: Polym. Chem.* **1992**, *30* (1), 125−132.
(33) Satoh, H.; Mineshima, A.; Nakamura, T.; Teramoto, N.; Shibata, M. Thermo-reversible Diels−Alder polymerization of difurfurylidene diglycerol and bismaleimide. *React. Funct. Polym.* **2014**, *76*, 49−56.
(34) Cioc, R. C.; Crockatt, M.; van der Waal, J. C.; Bruijnincx, P. C. A. The Interplay between Kinetics and Thermodynamics in Furan Diels−Alder Chemistry for Sustainable Chemicals Production. *Angew. Chem., Int. Ed.* **2022**, *61* (17), No. e202114720.
(35) Ravasco, J. M. J. M.; Gomes, R. F. A. Recent Advances on Diels-Alder-Driven Preparation of Bio-Based Aromatics. *ChemSusChem* **2021**, *14* (15), 3047−3053.
(36) Williamson, K. L.; Hsu, Y.-F. L.; Lacko, R.; Youn, C. H. Stereochemistry of the Diels-Alder reaction. syn-anti Isomerism. *J. Am. Chem. Soc.* **1969**, *91* (22), 6129−6138.
(37) Galkin, K. I.; Ananikov, V. P. Intermolecular Diels-Alder Cycloadditions of Furfural-Based Chemicals from Renewable Resources: A Focus on the Regio- and Diastereoselectivity in the Reaction with Alkenes. *Int. J. Mol. Sci.* **2021**, *22* (21), 11856.
(38) Alves, T. V.; Fernández, I. Understanding the reactivity and selectivity of Diels−Alder reactions involving furans. *Org. Biomol. Chem.* **2023**, *21* (38), 7767−7775.
(39) Taimoory, S. M.; Sadraei, S. I.; Fayoumi, R. A.; Nasri, S.; Revington, M.; Trant, J. F. Preparation and Characterization of a Small Library of Thermally-Labile End-Caps for Variable-Temperature Triggering of Self-Immolative Polymers. *J. Org. Chem.* **2018**, *83* (8), 4427−4440.
(40) Skolia, E.; Kokotos, C. G. Direct Diels-Alder Reaction of Biomass-Derived Furfurol with Maleimides in a Bio-Based Green Solvent. *Eur. J. Org. Chem.* **2024**, *27* (15), No. e202400105, DOI: 10.1002/ejoc.202400105.

(41) van der Loo, C. H. M.; Schim van der Loeff, R.; Martín, A.; Gomez-Sal, P.; Borst, M. L. G.; Pouwer, K.; Minnaard, A. J. π-Facial selectivity in the Diels−Alder reaction of glucosamine-based chiral furans and maleimides. *Org. Biomol. Chem.* **2023**, *21* (9), 1888−1894.
(42) Skolia, E.; Kokotos, C. G. Direct Diels-Alder Reaction of Biomass-Derived Furfurol with Maleimides in a Bio-Based Green Solvent. *Eur. J. Org. Chem.* **2024**, *27*, No. e202400105.
(43) Xu, F.; Li, Z.; Zhang, L.-L.; Liu, S.; Li, H.; Liao, Y.; Yang, S. Synthesis of renewable isoindolines from bio-based furfurals. *Green Chem.* **2023**, *25* (8), 3297−3305.
(44) Kamo, B.; Morita, I.; Horie, S.; Furusawa, S. Radical Polymerization of Furan with Maleic Anhydride through the Diels—Alder Adduct. *Polym. J.* **1974**, *6* (2), 121−131.
(45) Wang, T.; Gao, D.; Yin, H.; Zhao, J.; Wang, X.; Niu, H. Kinetic Study of the Diels−Alder Reaction between Maleimide and Furan-Containing Polystyrene Using Infrared Spectroscopy. *Polymers* **2024**, *16* (3), 441.
(46) Wilborn, E. G.; Gregory, C. M.; Machado, C. A.; Page, T. M.; Ramos, W.; Hunter, M. A.; Smith, K. M.; Gosting, S. E.; Tran, R.; Varney, K. L.; et al. Unraveling Polymer Structures with RAFT Polymerization and Diels−Alder Chemistry. *Macromolecules* **2019**, *52* (3), 1308−1316.
(47) Park, J.; Heo, J.-M.; Seong, S.; Noh, J.; Kim, J.-M. Self-assembly using a retro Diels-Alder reaction. *Nat. Commun.* **2021**, *12* (1), No. 4207.
(48) Castillo-Garcia, A. A.; Kappe, C. O.; Cantillo, D.; Barta, K. Aniline Derivatives from Lignin under Mild Conditions Enabled by Electrochemistry. *ChemSusChem* **2024**, *17* (3), No. e202301374.
(49) Lou, Y.; Marinkovic, S.; Estrine, B.; Qiang, W.; Enderlin, G. Oxidation of Furfural and Furan Derivatives to Maleic Acid in the Presence of a Simple Catalyst System Based on Acetic Acid and TS-1 and Hydrogen Peroxide. *ACS Omega* **2020**, *5* (6), 2561−2568.
(50) Ouyang, H.; Li, X.; Lu, X.; Xia, H. Selective Laser Sintering 4D Printing of Dynamic Cross-linked Polyurethane Containing Diels−Alder Bonds. *ACS Appl. Polym. Mater.* **2022**, *4* (5), 4035−4046.
(51) Zhou, Q.; Sang, Z.; Rajagopalan, K. K.; Sliozberg, Y.; Gardea, F.; Sukhishvili, S. A. Thermodynamics and Stereochemistry of Diels−Alder Polymer Networks: Role of Crosslinker Flexibility and Crosslinking Density. *Macromolecules* **2021**, *54* (22), 10510−10519.
(52) Duval, A.; Lange, H.; Lawoko, M.; Crestini, C. Reversible crosslinking of lignin via the furan−maleimide Diels−Alder reaction. *Green Chem.* **2015**, *17* (11), 4991−5000.
(53) Han, F.; Shi, Q.; Zhang, L.; Liu, B.; Zhang, Y.; Gao, Y.; Jia, R.; Zhang, Z.; Zhu, X. Stereoisomeric furan/maleimide adducts as latent monomers for one-shot sequence-controlled polymerization. *Polym. Chem.* **2020**, *11* (9), 1614−1620.
(54) Zhang, L.; Song, Y.; Cao, Y.; Wang, Z.; Huang, Z.; Xuan, S.; Zhang, Z. A photo−thermal dual-regulated latent monomer strategy for sequence control of polymers. *Polym. Chem.* **2021**, *12* (35), 4996−5002.
(55) Wang, J.; Chen, D.; Xing, S.; Ji, B.; Yang, J.; Tang, J. Highly Thermal Stable, Stiff, and Recyclable Self-Healing Epoxy Based on Diels−Alder Reaction. *ACS Appl. Polym. Mater.* **2024**, *6* (1), 466−474.
(56) Ganewatta, M. S.; Wang, Z.; Tang, C. Chemical syntheses of bioinspired and biomimetic polymers toward biobased materials. *Nat. Rev. Chem.* **2021**, *5* (11), 753−772.
(57) Oluwasanmi, A.; Hoskins, C. Potential use of the Diels-Alder reaction in biomedical and nanomedicine applications. *Int. J. Pharm.* **2021**, *604*, No. 120727.
(58) Gevrek, T. N.; Sanyal, A. Furan-containing polymeric Materials: Harnessing the Diels-Alder chemistry for biomedical applications. *Eur. Polym. J.* **2021**, *153*, No. 110514.
(59) Sancar, T.; Altinbasak, I.; Sanyal, R.; Sanyal, A. Electrospun photothermally active graphene-based nanofibers with a Retro-Diels-Alder reaction to initiate drug release. *Eur. Polym. J.* **2024**, *210*, No. 112946.
(60) Cerdan, K.; Thys, M.; Costa Cornellà, A.; Demir, F.; Norvez, S.; Vendamme, R.; Van den Brande, N.; Van Puyvelde, P.; Brancart, J. Sustainability of self-healing polymers: A holistic perspective towards circularity in polymer networks. *Prog. Polym. Sci.* **2024**, *152*, No. 101816.
(61) Ilochonwu, B. C.; van der Lugt, S. A.; Annala, A.; Di Marco, G.; Sampon, T.; Siepmann, J.; Siepmann, F.; Hennink, W. E.; Vermonden, T. Thermo-responsive Diels-Alder stabilized hydrogels for ocular drug delivery of a corticosteroid and an anti-VEGF fab fragment. *J. Controlled Release* **2023**, *361*, 334−349.
(62) Yan, J.; Jiang, W.; Kang, G.; Li, Q.; Tao, L.; Wang, X.; Yin, J. Synergistic chemo-photo anticancer therapy by using reversible Diels−Alder dynamic covalent bond mediated polyprodrug amphiphiles and immunoactivation investigation. *Biomater. Sci.* **2023**, *11* (17), 5819−5830.
(63) Li, F.; Li, X.; Zhang, X. Dynamic Diels−Alder reactions of maleimide−furan amphiphiles and their fluorescence ON/OFF behaviours. *Org. Biomol. Chem.* **2018**, *16* (42), 7871−7877.
(64) Peng, M.; Wang, Y.; Zhang, X. Pyrene-containing dyes: Reversible click/declick reaction, optical and aggregation behaviors. *Dyes Pigm.* **2020**, *179*, No. 108375.
(65) Cui, Y.; Li, F.; Zhang, X. Controlling fluorescence resonance energy transfer of donor−acceptor dyes by Diels−Alder dynamic covalent bonds. *Chem. Commun.* **2021**, *57* (26), 3275−3278.
(66) Vauthier, M.; Jierry, L.; Oliveira, J. C.; Hassouna, L.; Roucoules, V.; Bally-Le Gall, F. Interfacial Thermoreversible Chemistry on Functional Coatings: A Focus on the Diels−Alder Reaction. *Adv. Funct. Mater.* **2019**, *29* (10), No. 1806765.
(67) Tran, H. M.; Nguyen, L.-T. T.; Nguyen, T. H.; Nguyen, H. L.; Phan, N. T. S.; Zhang, G.; Yokozawa, T.; Tran, H. L.; Mai, P. T.; Nguyen, H. T. Efficient synthesis of a rod-coil conjugated graft copolymer by combination of thiol-maleimide chemistry and MOF-catalyzed photopolymerization. *Eur. Polym. J.* **2019**, *116*, 190−200.
(68) Nayab, S.; Trouillet, V.; Gliemann, H.; Weidler, P. G.; Azeem, I.; Tariq, S. R.; Goldmann, A. S.; Barner-Kowollik, C.; Yameen, B. Reversible Diels−Alder and Michael Addition Reactions Enable the Facile Postsynthetic Modification of Metal−Organic Frameworks. *Inorg. Chem.* **2021**, *60* (7), 4397−4409.
(69) Mondal, P.; Neuschuler, Z.; Mandal, D.; Hernandez, R. E.; Cohen, S. M. Reversible Postsynthetic Modification in a Metal−Organic Framework. *Angew. Chem., Int. Ed.* **2024**, *63* (9), No. e202317062.
(70) Kucherov, F. A.; Galkin, K. I.; Gordeev, E. G.; Ananikov, V. P. Efficient route for the construction of polycyclic systems from bioderived HMF. *Green Chem.* **2017**, *19* (20), 4858−4864.
(71) *Gaussian 09*; Gaussian, Inc.: Wallingford CT, 2016.
(72) Martin, J. G.; Hill, R. K. Stereochemistry of the Diels-Alder Reaction. *Chem. Rev.* **1961**, *61* (6), 537−562.
(73) Taherinia, D.; Fattahi, A. Inducing high exo selectivity in Diels−Alder reaction by dimethylborane substituent: a DFT study. *Sci. Rep.* **2022**, *12* (1), No. 22225.
(74) Iuliano, V.; Talotta, C.; Gaeta, C.; Hickey, N.; Geremia, S.; Vatsouro, I.; Kovalev, V.; Neri, P. Influence of exo-Adamantyl Groups and endo-OH Functions on the Threading of Calix[6]arene Macrocycle. *J. Org. Chem.* **2020**, *85* (19), 12585−12593.

https://doi.org/10.1021/acsomega.4c03804
ACS Omega 2024, 9, 36380−36388